

Sub-barrier and near-barrier fusion study of halo nuclei

N. Alamanos,¹ A. Pakou,² V. Lapoux,¹ J. L. Sida,¹ and M. Trotta³

¹DSM/DAPNIA CEA SACLAY, F-91191 Gif-sur-Yvette, France

²Department of Physics, The University of Ioannina, GR-45110 Ioannina, Greece

³INFN, Laboratori Nazionali di Legnaro, via Romea 4, I-35020 Legnaro, Padova, Italy

(Received 23 January 2002; published 25 April 2002)

The near-barrier and sub-barrier fusion of light unstable nuclei and their respective stable isotopes with heavy targets (${}^4\text{He}+{}^{209}\text{Bi}$, ${}^4\text{He}+{}^{238}\text{U}$, ${}^9\text{Be}+{}^{209}\text{Bi}$, and ${}^9\text{Be}+{}^{208}\text{Pb}$) is investigated via coupled channel calculations. The entrance channel optical potential is generated via a microscopic BDM3Y1 interaction. A rather satisfactory description of the experimental data is obtained under the condition that the real part of the optical potential has to be reduced for the weakly bound and halo systems. This reduction proves to be the fundamental difference in treating stable and weakly bound nuclei, and can be attributed to the loss of a flux due to breakup effects.

DOI: 10.1103/PhysRevC.65.054606

PACS number(s): 25.70.Jj, 25.60.Gc, 24.10.Eq

I. INTRODUCTION

Several experimental and theoretical studies concerning the fusion of two nuclei under and near the Coulomb barrier were performed in the past [1]. Most of the results were interpreted adequately well within the framework of coupled-channel (CC) calculations and by using either microscopic potentials or phenomenological ones [2,3]. With the advent of radioactive beam facilities, the interest in such studies with halo nuclei was renewed due to their specific features, like extended neutron densities, low-lying continuum, and also very low-energy thresholds for breakup. Fusion, like other reaction processes, should be appreciably affected by such features. The experimental results obtained for fusion reactions at energies close to the Coulomb barrier with light unstable beams were recently reviewed by Signorini [4]. The data point out a strong influence due to breakup processes.

From a theoretical point of view, it is expected that fusion cross sections for halo nuclei will present an increase due to the decrease of the potential barrier and the coupling to soft vibrational modes [5]. This increase, however, according to several elaborate but contradictory theories [6–12], may be hindered or enhanced due to breakup effects.

In this work near-barrier and sub-barrier fusion of halo nuclei and weakly bound stable nuclei will be explored through CC calculations for various degrees of freedom. The influence of breakup will be anticipated via an “appropriate” potential. The structure of the colliding nuclei will be taken into account explicitly via a folding process. Traditionally the optical potential is inferred through elastic-scattering results. The overall success of realistic folding models for the description of elastic-scattering data of stable nuclei, without any renormalization N of the real potential (N is close to unity), is well known, indicating that the real dynamic polarization potential (DPP) is weak [13]. On the other hand, a dramatic differentiation occurs for the scattering of weakly bound nuclei [13–15] due to the breakup effects. In fact, data for ${}^6\text{Li}$ and ${}^9\text{Be}$ nuclei on various targets required a substantial renormalization of the real folded potential by a factor of $N\sim 0.6$, while for the system ${}^9\text{Be}+{}^{208}\text{Pb}$ the normal-

ization factor N was equal to 0.36 [13,16]. In an alternative way the effect of breakup in elastic scattering was studied explicitly by Sakuragi [17] in the framework of discretized CC calculations, without any renormalization of the folding real potential.

Consequently, it is clear to us that two types of calculations can anticipate the breakup effect in elastic scattering, through which we can obtain the appropriate potential to describe near-barrier and sub-barrier fusion. The first is the method of discretized CC calculations, [17,18], which is probably the most accurate method but at the same time depends on several parameters. The second one involves a reduced real potential, which is a local representation (not exact) of the discretized CC calculations, in the sense that by solving a one-channel Schrödinger equation with that reduced potential, the same results are obtained as the ones with CC calculations [15]. In our study we will apply the second method, keeping in mind that coupling to the continuum may not be fully represented by a simple reduction of the depth of the entrance channel potential, since the real part of the DPP may not have the same radial shape as the folded one [15,19].

II. SYSTEMATICS OF PREVIOUS EXPERIMENTAL RESULTS

Before the presentation of our calculations we will try to compare existing data for unstable nuclei and their respective stable isotopes, to point out any similarities and differences which they may shed light in our analysis. The first measurements with halo nuclei were performed for the systems ${}^{11}\text{Be}+{}^{209}\text{Bi}$ [20], ${}^6\text{He}+{}^{209}\text{Bi}$ [21], and ${}^6\text{He}+{}^{238}\text{U}$ [22]. The data are presented in Fig. 1 together with the data of the respective stable isotopes ${}^9\text{Be}+{}^{209}\text{Bi}$ [20], ${}^4\text{He}+{}^{209}\text{Bi}$ [23], and ${}^4\text{He}+{}^{238}\text{U}$ [22,24].

For ${}^9\text{Be}+{}^{209}\text{Bi}$ and ${}^4\text{He}+{}^{209}\text{Bi}$ the detection of the fusion products was carried out via their characteristic delayed α -particle activities. Conversely, for ${}^4\text{He}+{}^{238}\text{U}$ the fission cross section was measured. Fission can be also triggered by inelastic or transfer reaction events. In such cases the fission would be accompanied by a residue of the projec-

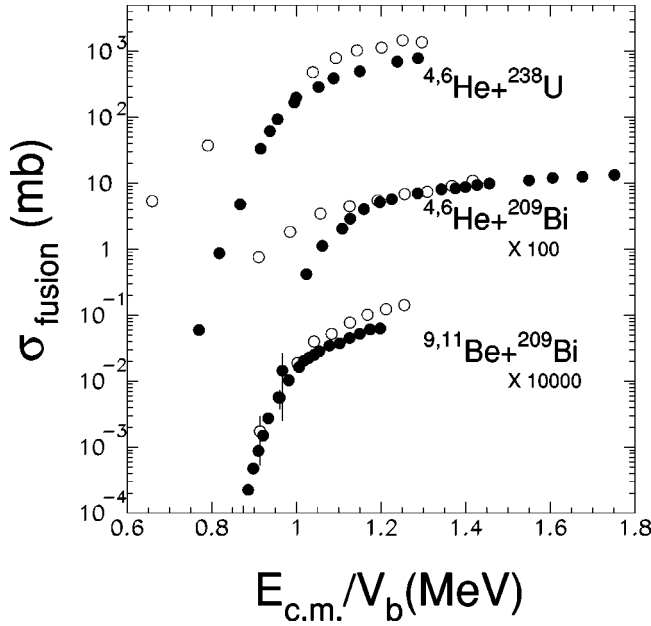


FIG. 1. Comparison of fusion cross-section measurements for the halo system (open circles) and the respective stable systems (closed circles). The data are from Refs. [20–24].

tile. It was verified that contributions corresponding to multiplicity equal to three were very small [22]. It was assumed, therefore, that around the Coulomb barrier the fission cross section was very close to fusion cross section.

Special attention has to be paid, comparing the systems ${}^6\text{He}+{}^{209}\text{Bi}$ and ${}^4\text{He}+{}^{209}\text{Bi}$. The compound nucleus ${}^{215}\text{At}$ formed via the ${}^6\text{He}+{}^{209}\text{Bi}$ fusion reaction decays exclusively by evaporation of two, three, or four neutrons. The total fusion cross section for the system ${}^6\text{He}+{}^{209}\text{Bi}$ was obtained by adding the $3n$ and $4n$ channels. The effect of the $2n$ channel is small except at energies well below the barrier [21]. In this respect, it is compared to the ${}^4\text{He}+{}^{209}\text{Bi}$ fusion cross section obtained by adding the $2n$, $3n$, and $4n$ channels, which makes this comparison meaningful. As will be shown later on, to obtain the total fusion cross section for the system ${}^4\text{He}+{}^{209}\text{Bi}$, one has to add the $1n$ channel. Cross sections are presented in Fig. 1 as a function of energy divided by the Coulomb barrier V_b . Barriers were extracted via the relations of Christensen and Winther [25], and are shown in Table I. The presentation of all the data in Fig. 1 facilitates the extraction of the following conclusions. For energies higher than the Coulomb barrier the cross sections for the fusion of ${}^{9,11}\text{Be}+{}^{209}\text{Bi}$ and ${}^{4,6}\text{He}+{}^{238}\text{U}$ present the same behavior. That is, the cross sections for halo projectiles are enhanced over the cross sections for the stable ones. On the other hand, no apparent enhancement is seen for the fusion of the ${}^6\text{He}$ over that of ${}^4\text{He}$ on the ${}^{209}\text{Bi}$ target. For energies lower than the Coulomb barrier, the fusion cross section for the halo nucleus ${}^6\text{He}$ on ${}^{238}\text{U}$ and ${}^{209}\text{Bi}$ targets is enhanced over that of ${}^4\text{He}$, while no such enhancement is observed for the fusion of the ${}^{11}\text{Be}$ on ${}^{209}\text{Bi}$ over that of ${}^9\text{Be}$.

TABLE I. Coulomb heights V_b (MeV) according to (A) Christensen and Winther, (B) the BDM3Y1 potential, and (C) the BDM3Y1 potential reduced by 40% in all cases except for the ${}^9\text{Be}+{}^{208}\text{Pb}$ system, where the reduction was $\sim 60\%$.

System	A	B	C
${}^4\text{He}+{}^{238}\text{U}$	22.61 ± 0.2	22.48 ± 0.2	
${}^4\text{He}+{}^{209}\text{Bi}$	20.90 ± 0.2	21.34 ± 0.2	
${}^9\text{Be}+{}^{209}\text{Bi}$	39.95 ± 0.2	38.44 ± 0.2	39.92 ± 0.2
${}^9\text{Be}+{}^{208}\text{Pb}$	39.52 ± 0.2	36.95 ± 0.2	40.06 ± 0.2
${}^6\text{He}+{}^{238}\text{U}$	22.14 ± 0.2	19.51 ± 0.2	20.37 ± 0.2
${}^6\text{He}+{}^{209}\text{Bi}$	20.47 ± 0.2	18.18 ± 0.2	19.10 ± 0.2
${}^{11}\text{Be}+{}^{209}\text{Bi}$	35.68 ± 0.2	35.68 ± 0.2	37.40 ± 0.2

III. ANALYSIS

Subsequently we proceeded with a consistent analysis of all the above systems. For completeness the system ${}^9\text{Be}+{}^{208}\text{Pb}$ [26] was also included, although no data exist for its associate halo system. The aim was to describe all the encountered systems, either stable or weakly bound or unstable, within the same framework, taking advantage of the similarities between weakly bound and unstable systems and trying to unveil interesting aspects in physics that may emerge from fusion measurements with halo nuclei.

In this context, coupled channel calculations were performed with the ECIS code [27]. The real part of the entrance potential was calculated within the double folding model [13] by using the BDM3Y1 interaction developed by Khoa *et al.* [28]. This interaction was found before [16,29] to describe rather well elastic-scattering data for both stable and weakly bound nuclei, as long as the normalization factor for the weakly bound ones is substantially reduced. We note that, in the present analysis the normalization factor of the entrance potential was set equal to unity ($N=1$) for the stable isotopes. We have set the normalization factor for all stable weakly bound and halo nuclei equal to $N=0.6$, following the general trend of the weakly bound systems [16], with the exception of ${}^9\text{Be}+{}^{208}\text{Pb}$, where the normalization factor was set equal to $N=0.36$ according to existing elastic scattering data [13]. The adopted imaginary potential was such as to absorb all the flux penetrating the barrier, simulating the incoming wave boundary condition. The stability of the optical-model calculations was studied at an energy slightly below the barrier as a function of the imaginary potential parameters. In fact it was observed that for an imaginary potential depth higher than 10 MeV and a radius smaller than 0.8 fm, the calculated fusion cross sections are practically constant.

The densities involved in the real double folded potential for the stable isotopes were obtained from electron-scattering data by adopting standard procedures [13]. For the radioactive nuclei shell model densities [30], and HF densities [31] were used for ${}^6\text{He}$ and ${}^{11}\text{Be}$, respectively.

The BDM3Y1 potential barriers, obtained in the present analysis for $N=1$, are shown in Table I. It is obvious that

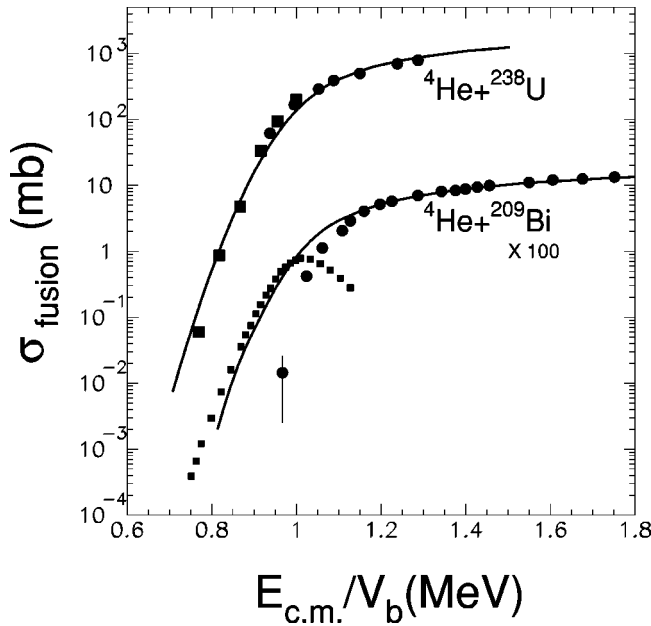


FIG. 2. Fusion cross-section measurements for stable nuclei are compared with CC calculations with a nonreduced optical potential. The data for the system ${}^4\text{He}+{}^{238}\text{U}$ indicated by solid circles come from Ref. [22], and those indicated with solid boxes from Ref. [24]. The data for the system ${}^4\text{He}+{}^{209}\text{Bi}$ indicated by solid circles come from Ref. [23] and refer to a sum of the $2n$, $3n$, and $4n$ evaporation channels, while data indicated by solid boxes come from Ref. [34] and refer to the $1n$ evaporation channel.

barrier heights of the systems with weakly bound nuclei present a reduction of ~ 3 MeV relatively to the heights of the systems with their associated stable isotopes. This is a well-known effect, a quantitative understanding of which has been achieved in terms of the halo structure [5]. The consequence of a reduced height is the enhancement of the sub-barrier fusion cross sections, sometimes by a few orders of magnitude.

The calculation for the system ${}^4\text{He}+{}^{238}\text{U}$ has been performed within the rotational model. Couplings to the first excited states of ${}^{238}\text{U}$ were considered with deformations extracted from $B(E2)$'s reported previously [32]. In addition to our previous calculation [22] we have used now not only multipolarities with $\lambda=2$ but also with $\lambda=4$. The calculation for the system ${}^4\text{He}+{}^{209}\text{Bi}$ includes couplings to the two excited states of ${}^{209}\text{Bi}$, $E=0.896$ MeV ($\lambda=2$) and $E=1.608$ MeV ($\lambda=3$), with deformations reported in the compilation [33]. For these two systems we have considered only couplings to the target excitations. The calculations are compared with the experimental data in Fig. 2. We point out that the additional data, indicated in Fig. 2 with squares, correspond to the $1n$ evaporation channel of the reaction ${}^{209}\text{Bi}(\alpha,n){}^{212}\text{At}$ [34]. As expected, the experimental results of both systems can be reproduced equally well within our theoretical framework, and without any reduction of the potential.

Using similar calculations we proceeded with the analysis of the ${}^9\text{Be}+{}^{209}\text{Bi}$ and ${}^9\text{Be}+{}^{208}\text{Pb}$ systems with weakly

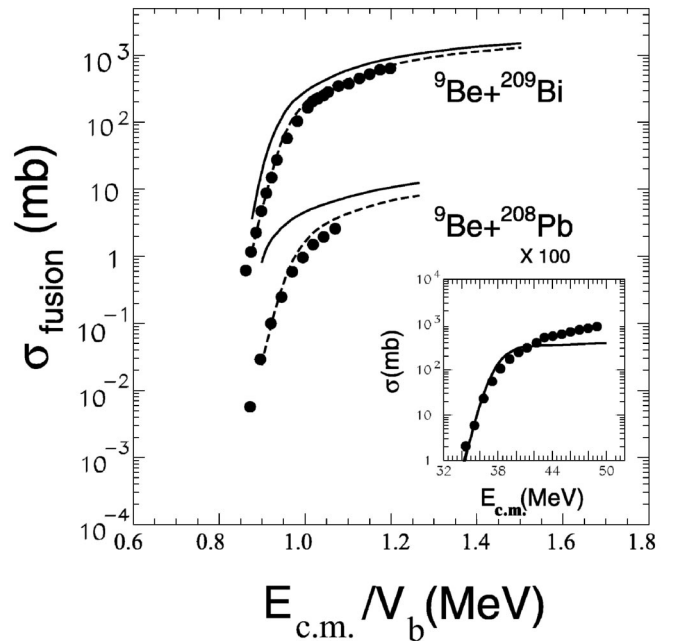


FIG. 3. Fusion cross-section measurements for weakly bound systems are compared with CC calculations with a nonreduced ($N=1$) optical potential (solid line) and a reduced optical potential ($N=0.6$ and 0.36 for the ${}^9\text{Be}+{}^{209}\text{Bi}$ and ${}^9\text{Be}+{}^{208}\text{Pb}$, correspondingly) (dashed line). In the inset cross-section breakup measurements for the system ${}^9\text{Be}+{}^{208}\text{Pb}$ are compared with calculated values obtained as the difference between cross sections with reduced and nonreduced optical potentials.

bound projectiles and then to the systems ${}^6\text{He}+{}^{209}\text{Bi}$, ${}^{11}\text{Be}+{}^{209}\text{Bi}$, ${}^6\text{He}+{}^{238}\text{U}$ with halo projectiles. For the system ${}^9\text{Be}+{}^{209}\text{Bi}$, we have taken into account additionally to the excited states of ${}^{209}\text{Bi}$, the excited states of ${}^9\text{Be}$, $E=1.680$ MeV ($\lambda=1$) and 2.430 MeV ($\lambda=2$). The $B(E1)$ and $B(E2)$ values for the transitions to these states were recently obtained by Rudchik *et al.* [35]. For the system ${}^9\text{Be}+{}^{208}\text{Pb}$ we have considered the well-known low-lying states of ${}^{208}\text{Pb}$ [36], $E=2.62$ MeV ($\lambda=3$) and $E=4.09$ ($\lambda=2$) and the excited states of ${}^9\text{Be}$ as above. The calculations (solid lines for nonreduced potential and the dashed line for a reduced potential), are compared with the experimental data in Fig. 3. As can be seen, the adopted reduction of the potential according to the elastic scattering data (40% for the ${}^9\text{Be}+{}^{209}\text{Bi}$ system and 60% for the ${}^9\text{Be}+{}^{208}\text{Pb}$ one) was adequate to describe very well the sub-barrier and near-barrier fusion data. As is seen, moving to weakly bound nuclei, a potential reduction is necessary to simulate the flux loss through the breakup channel. A justification of this reduction is given in the inset of Fig. 3, where breakup cross sections are compared with calculations obtained as the difference between results with full potential and reduced potential. We should clear up this point. Breakup can result from several different reaction mechanisms including direct breakup, sequential breakup via inelastic excitation, and nucleon transfer followed by breakup, among others. In any case, it corresponds to the flux which does not lead to fusion.

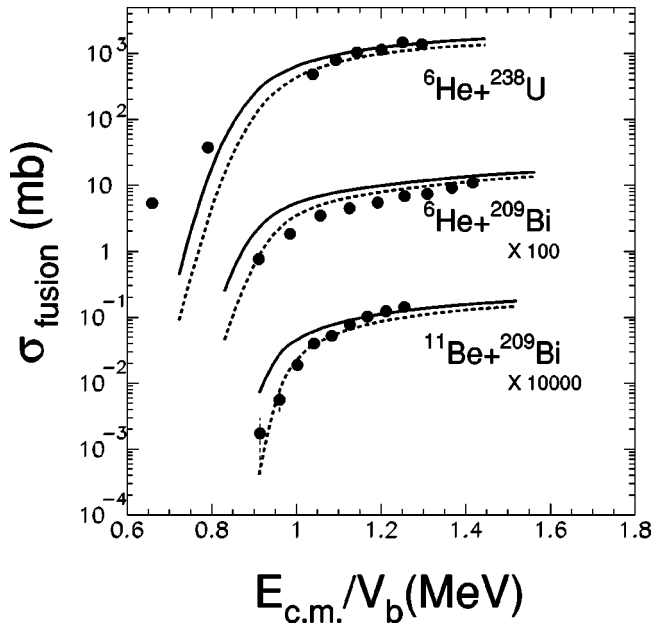


FIG. 4. Fusion cross-section measurements for halo systems are compared with CC calculations with a nonreduced ($N=1$) optical potential (solid line) and a reduced ($N=0.6$) optical potential (dashed line).

For the halo projectile systems, coupling to the excited states of the ^{209}Bi and ^{238}U targets was taken as before. Coupling to the excited states of the projectiles was considered as follows: for ^6He we considered the coupling to the first excited state at 1.79 MeV ($\lambda=2$), with deformation extracted from our recent inelastic scattering results $^6\text{He}(p,p')^6\text{He}$ [37]; for ^{11}Be the excited state $E=0.320$ MeV ($\lambda=1$) with a $B(E1)=0.116e^2\text{ fm}^4$ was taken into account. The calculations are compared with the experimental data in Fig. 4. A qualitative overall agreement is obtained for all the systems with a 40% reduction of the potential. On the other hand, for energies well above the Coulomb barrier, the $^{11}\text{Be}+^{209}\text{Bi}$ system is better described with nonreduced potential calculations. The situation is more complex for $^6\text{He}+^{238}\text{U}$. Above the Coulomb barrier this system is probably better described with calculations with a nonreduced potential, whereas well below the Coulomb barrier the calculations fail to reproduce the data [38].

IV. CONCLUSIONS

From the present analysis we can draw the conclusion that the CC calculations, taking into account the breakup effects via a reduced potential in a simple way, reproduce the gross properties of near-barrier and sub-barrier fusion of weakly bound nuclei with heavy targets. The agreement of the calculations with the data is particularly spectacular in the case of the systems $^9\text{Be}+^{209}\text{Bi}$ and $^9\text{Be}+^{208}\text{Pb}$, where the exact reduction of the potential was known from elastic-scattering data [13,16] at energies well above the Coulomb barrier. For the unstable systems the situation seems to be more compli-

cated, probably due to the lack of elastic scattering results at energies well above the Coulomb barrier. Therefore, predictions of fusion with halo nuclei remains in a qualitative basis.

Here we would also like to underline the importance of a precise knowledge of the entrance channel optical potential for the analysis of sub-barrier fusion results. Indeed, it is well known from the elastic scattering of stable nuclei that an anomaly occurs around the Coulomb barrier which is visualized by a rapid variation of the optical potential: an increase of the real and decrease of the imaginary potential. This anomaly is attributed to CC effects, and is taken implicitly into account in CC calculations [39]. In an alternative way near-barrier and sub-barrier fusion cross sections can be described by using a one-dimensional barrier penetration model and an energy-dependent potential, taking into account the threshold anomaly [39,40]. However, in the case of weakly bound nuclei, couplings between breakup and elastic channels give rise to a large repulsive real polarization potential, as assumed in the present analysis, and to a very weak imaginary potential that is almost energy independent. Therefore, loosely bound nuclei may not display a threshold anomaly, as suggested by Mahaux, Ngô, and Satchler [41] and reported in the case of ^6Li [42,43]. In this context, more elastic-scattering data for weakly bound systems and halo nuclei and more elaborate methods are probably necessary to incorporate breakup effects in sub-barrier fusion calculations through potentials deduced from elastic-scattering data at energies close to the Coulomb barrier.

In summary, we have performed CC fusion calculations for several systems with halo projectiles and their respective nonhalo projectiles. It was found that a fundamental difference occurs between stable and unstable systems. The dominant channel in the barrier energy region of stable systems is fusion. For unstable and weakly bound nuclei this is not the case. Losses of the flux through other channels like breakup take place, and can be taken into account by the reduction of the real part of the entrance channel optical potential, i.e., exactly in the same way as for elastic-scattering data. In that respect, the description of the weakly bound systems—($^9\text{Be}+^{209}\text{Bi}$), ($^9\text{Be}+^{208}\text{Pb}$) and the halo systems—($^6\text{He}+^{209}\text{Bi}$), ($^6\text{He}+^{238}\text{U}$), and ($^{11}\text{Be}+^{209}\text{Bi}$)—were adequately obtained, by making use of a reduced potential to account for the breakup processes. Although for the weakly bound systems this description was excellent, for the halo systems only a qualitative agreement was obtained. More elaborate theoretical approaches and additional measurements including elastic scattering, complete fusion (without contributions due to incomplete fusion) and breakup are necessary, in order to obtain a more comprehensive picture of near-barrier and sub-barrier fusion, involving halo nuclei.

ACKNOWLEDGMENTS

One of the authors (N.A.) would like to express his sincere thanks to Dr. F. Auger, Dr. A. Gillibert, and Dr. D. Ridikas for many useful discussions.

- [1] M. Beckerman, Rep. Prog. Phys. **51**, 1047 (1988).
- [2] S. G. Steadman and M. J. Rhoades-Brown, Annu. Rev. Nucl. Part. Sci. **36**, 649 (1986).
- [3] G. Pollarolo and A. Winther, Phys. Rev. C **62**, 054611 (2001).
- [4] C. Signorini, Nucl. Phys. **A693**, 190 (2001).
- [5] N. Takigawa and H. Sagawa, Phys. Lett. B **265**, 23 (1991).
- [6] M. S. Hussein and M. P. Pato, Phys. Rev. C **46**, 377 (1992).
- [7] C. H. Dasso and A. Vitturi, Phys. Rev. C **50**, R12 (1994).
- [8] N. Takigawa, M. Kuratani, and H. Sagawa, Phys. Rev. C **47**, R2470 (1993).
- [9] M. S. Hussein *et al.*, Phys. Rev. C **46**, 377 (1992).
- [10] M. S. Hussein and A. F. de Toledo Piza, Phys. Rev. Lett. **72**, 2693 (1994).
- [11] M. S. Hussein and A. F. de Toledo Piza, Phys. Rev. C **51**, 846 (1995).
- [12] K. Hagino *et al.*, Phys. Rev. C **61**, 037602 (2000).
- [13] G. R. Satchler and W. G. Love, Phys. Rep. **55**, 183 (1979).
- [14] C. B. Fulmer *et al.*, Nucl. Phys. **A427**, 545 (1984).
- [15] M. E. Brandan and G. R. Satchler, Phys. Rep. **285**, 143 (1997).
- [16] L. Trache *et al.*, Phys. Rev. C **61**, 024612 (2000).
- [17] Y. Sakuragi, Phys. Rev. C **35**, 2161 (1987).
- [18] M. S. Hussein *et al.*, Phys. Rev. C **29**, 2383 (1984).
- [19] V. Lapoux *et al.*, Phys. Lett. B **517** 18 (2001); Ph.D. thesis, University of Orsay, 1998.
- [20] C. Signorini *et al.*, Eur. Phys. J. A **227**, 157 (1998).
- [21] J. J. Kolata *et al.*, Phys. Rev. C **81**, 4580 (1998).
- [22] M. Trotta *et al.*, Phys. Rev. Lett. **84**, 2342 (2000).
- [23] W. J. Ramler *et al.*, Phys. Rev. **114**, 154 (1959).
- [24] V. E. Viola and T. Sikkeland, Phys. Rev. **128**, 767 (1962).
- [25] P. R. Christensen and W. Winter, Phys. Lett. **65B**, 19 (1976).
- [26] M. Dasgupta *et al.*, Phys. Rev. Lett. **82**, 1395 (1999).
- [27] J. Raynal, Phys. Rev. C **23**, 2571 (1981).
- [28] D. T. Khoa *et al.*, Phys. Lett. B **342**, 6 (1995).
- [29] D. T. Khoa, G. R. Satchler, and W. von Oertzen, Phys. Rev. C **56**, 954 (1997).
- [30] S. Karataglidis *et al.*, Phys. Rev. C **61**, 024319 (2000); (private communication).
- [31] H. Sagawa, Phys. Lett. B **286**, 7 (1992).
- [32] F. K. McGowan *et al.*, Phys. Rev. Lett. **27**, 1741 (1971).
- [33] M. J. Martin, Nucl. Data Sheets **63**, 723 (1991).
- [34] A. R. Barnett and J. L. Lilley, Phys. Rev. C **9**, 2010 (1974).
- [35] A. T. Rudchik *et al.*, Nucl. Phys. **A662**, 44 (2000).
- [36] R. Liguori-Neto *et al.*, Nucl. Phys. **A560**, 733 (1993).
- [37] A. Lagoyannis *et al.*, Ph.D. thesis, University of Ioannina, 2001.
- [38] E. F. Anguilera *et al.*, Phys. Rev. Lett. **84**, 5058 (2000).
- [39] G. R. Satchler *et al.*, Ann. Phys. (N.Y.) **178**, 110 (1987).
- [40] M. A. Nagarajan and G. R. Satchler, Phys. Lett. B **173**, 29 (1986).
- [41] C. Mahaux, H. Ngô, and G. R. Satchler, Nucl. Phys. **A449**, 354 (1986).
- [42] N. Keeley *et al.*, Nucl. Phys. **A571**, 326 (1994).
- [43] M. A. Tide *et al.*, Phys. Rev. C **44**, 1698 (1991).